

Segmental Dynamics of Reactively Prepared Polystyrene Blends: Unsaturated Polyester Resin Versus High Impact Polystyrene

N. Taheri Qazvini,* N. Mohammadi

Loghman Fundamental Research Group, Polymer Engineering Department, Amirkabir University of Technology, Tehran, Iran

Received 31 August 2005; accepted 5 August 2006

DOI 10.1002/app.26365

Published online 26 June 2007 in Wiley InterScience (www.interscience.wiley.com).

ABSTRACT: Segmental dynamics of two phase-separated reactively prepared polystyrene blends namely unsaturated polyester resin (UPR) and high impact polystyrene (HIPS) was investigated by dynamic-mechanical spectroscopy and calorimetric studies. The results showed a thermorheologically simple behavior for the HIPS, which could be quantified based on the KWW function with β_{KWW} of 0.37. The UPR data, however, could not be evaluated using KWW function, even though lower β_{KWW} than the HIPS was expected for it. Furthermore, the α -dispersion of the UPR was considerably broader while its fragility index was comparable with the HIPS. Nonetheless, segmental dynamics comparison based on normalized $\Delta C_p(T_g)$ by molecular

weight of the structural units of the studied systems showed much greater differences. Accordingly, the UPR was both kinetically and thermodynamically more fragile than the HIPS. The higher fragility of the UPR could be attributed to its larger relative cooperativity size and topological constraints. Finally, enhanced contrast in dynamic fragilities of two studied systems could be achieved if similar overall and local compositions could be made experimentally. © 2007 Wiley Periodicals, Inc. *J Appl Polym Sci* 106: 498–504, 2007

Key words: segmental dynamics; unsaturated polyester; high impact polystyrene; glass transition; fragility

INTRODUCTION

Tuning of the macroscopic properties of polymers based on appreciation of their microscopic chain dynamics have been the motives for many research works.^{1–6} A common theme, explicit or implied, has been that mechanical stress field may provoke the same molecular motions as would normally appear as a result of thermal fluctuation at higher temperatures. For example, the physical origin of the plastic deformation in polymers is large-scale cooperative motions similar to those responsible for the glass transition phenomenon.^{4–6} Accordingly, when a mechanical force is applied on a chain through its surrounding, its segments readjust themselves to relieve the stress. Therefore, the momentarily raised free energy is dissipated by a small amount every time a segment reorients itself to a new state with lower free energy.¹

As a generally accepted picture, however, glass transition engages in complete rotational relaxation,

which requires cooperativity of the neighboring units to overcome the intermolecular barriers.^{4–9} In other words, a constrained structural unit can change its conformational state only if its close neighbors cooperate as if they are in a set of meshed components. A great deal of attention has been devoted looking for adequate approaches to highlight the universal features of glass-forming systems. For example, many research works have focused on the temperature-dependence of the average relaxation time.^{7–10} Accordingly, supercooled liquids can be classified as “strong” and “fragile.”¹⁰ Strong systems display an Arrhenius-type temperature-dependence and relatively small changes in their heat capacity at the glass transition temperature, T_g . On the other hand, the fragile systems are characterized by their pronounced relaxation time-temperature deviations from Arrhenius behavior and large liquid to glass heat capacity ratios at T_g .^{10,11} Therefore, the steepness of semilogarithmic plots of relaxation time versus T_g/T , fragility, provides a measure of relative temperature sensitivity and compares materials directly. To cast a universal view, however, fragility has been related to the chemical structure of materials.^{7,12,13} Polymers, containing smooth, compact, and symmetrical chains exhibit strong relaxation behavior, while fragile polymers are made of more rigid backbones or sterically hindering pendant groups.¹² These microstructure-based charac-

Correspondence to: N. Mohammadi (mohamadi@aut.ac.ir).

*Present address: School of Chemistry, University College of Science, University of Tehran, Tehran, Iran

Contract grant sponsor: Loghman Fundamental Research Group.

teristics reflect the topology, that is, the number of minima and the barrier height between them, with certain potential energy landscapes,¹⁰ which govern segmental rearrangement of polymers. Strictly speaking, the height of the energy barriers and the number of minima imply the kinetic and thermodynamic aspects of chain dynamics, respectively.⁸

In case of multicomponent polymer systems, however, cooperative configurational rearrangements may involve segments pertaining to similar or different molecules depending on the compositional scale of heterogeneity. In thermodynamically miscible blends, the components dynamic exhibit different temperature-dependencies. In other words, at any given temperature, the relaxation of the high- T_g and low- T_g components becomes faster or slower in comparison with their pure state, respectively. Accordingly, the system does not follow the time-temperature superposition principle. Some workers^{14,15} attributed this to the blend dynamic heterogeneity originating from existing concentration fluctuations. However, others considered the effect of monomer connectivity on its local enrichment in mean blend composition (self-concentration model)¹⁶ or used the combined effects of both phenomena.¹⁷ Quite recently, Ediger and coworkers¹⁸ showed that in miscible polymer blends even in dilute regime, the segmental dynamics of isolated chains did not become slaved to the host matrix. Accordingly, they confirmed the preference of self-concentration model in rationalizing miscible polymer blends dynamics.

Nonetheless, many polymeric blend systems are immiscible to some extent with many diversified applications. For example, incorporation of rubbery or glassy inclusions into the brittle polymers as a biphasic structure modifies the ligament, the matrix between modifier particles, and leads to enhanced properties. Historically, high impact polystyrene (HIPS) and unsaturated polyester resin (UPR) are prepared via polymerizing the styrene solution containing an unsaturated polymer (polybutadiene or polyester) leading to phase-separated systems with polystyrene as the continuous phase. In HIPS and UPR, micron size stiff (polybutadiene domains with polystyrene inclusions) and rigid particles (conterminously bonded polyester microgels) are distributed in polystyrene matrix, respectively. However, the important question of the molecular basis for observing the enhanced properties by the inclusion of secondary phase particles remains for further studies and elaborations.

In this work, the non-Arrhenius behavior of commercial HIPS and UPR were investigated in the glass-transition region by dynamic mechanical analysis and differential scanning calorimetry. Furthermore, their temperature-dependence of the relaxation times and the length scale of cooperative motions were compared by applying the fragility concept.

EXPERIMENTAL

The UPR was provided by Bushehr resin. The resin is made of maleic anhydride (MA), phthalic anhydride (PA), and propylene glycol (PG) (0.5 : 0.5 : 1.1) as determined by ¹H NMR. The styrene monomer was supplied by an industry and used as received. The amount of styrene in the resin was determined by its evaporation in an air-circulating oven at 110°C for 2 h. Then, a sample with 60% (w/w) styrene was prepared by diluting the resin with styrene via mixing them for 1 h at ambient temperature. Later, 0.5% (w/w) cobalt octate (Activator) was dissolved in the mixture.

Plates, 2 mm in thickness, were cast from the resin mixture. Curing was initiated at room temperature by adding 1% (w/w) methyl-ethyl-ketone peroxide as a catalyst to the mixture. The thermal cycle of curing was consisted of isothermal heating at 25°C for 24 h, followed by postcuring at 80°C for 8 h and 120°C for 2 h.¹⁹ Thermogravimetric analysis on final cured resins showed almost complete chemical transformation (less than 0.5% (w/w) unreacted monomer was detected).

A bulk polymerized high-impact polystyrene, HIPS (Tabriz Petrochemical Co. 4240), containing 7% (w/w) of butadiene rubber was used. The volume fraction of the dispersed composite rubber particles (with polystyrene inclusions) was estimated to be about 20% (v/v).²⁰ The weight-average molecular weight of the polystyrene matrix was 1.9×10^5 g/mol with a polydispersity of 3.2. Sheets, 2 mm in thickness, were compression-molded at 190°C and 4 MPa.

Dynamic-mechanical analysis was performed by a TA Instrument, DMA-2980, at both isothermal (frequency sweep) and nonisothermal (temperature scan) conditions for all samples in bending mode. Dual cantilever clamp was used on samples with rectangular geometry of 50×13 mm². The nonisothermal runs were carried out at 4°C/min from room temperature up to 200°C at constant frequency of 3 Hz. The frequency sweep experiments, however, were carried out in the glass transition region (determined by nonisothermal runs) for each sample at 2–4°C intervals after temperature equilibration for 20 min. At each temperature, the frequency was changed from 200 to 0.01 Hz.

Differential scanning calorimetry (TA instrument, DSC 2010) was used to measure the specific heat capacities against a sapphire standard. A blank pan was run immediately prior to characterization of each polymer sample. The calibration of instrument was checked based on the melting point of indium after each six measurements. For each sample, about 10 mg of material was sealed in an aluminum pan and run in all DSC experiments. The thermograms were taken on the second heating (10 K/min) cycle after quenching from elevated temperature. Samples were annealed

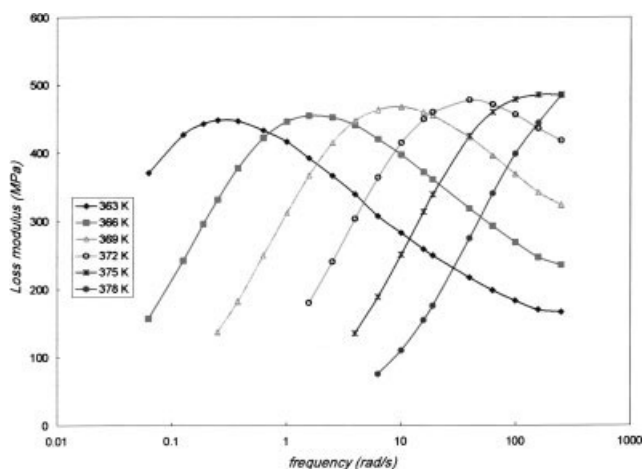


Figure 1 DMA isothermal curves for the HIPS at different temperatures in the glass transition region.

for at least 40 min at 200°C before quenching to erase prior thermal histories. The reported heat capacities are averages of three runs.

RESULTS AND DISCUSSION

Viscoelastic data of the studied systems in the α -relaxation region are plotted in Figures 1 and 2. For both systems, the loss peak shifts to higher temperatures as the test frequency increases. Approximate superposition of the loss peaks based on normalization to the maximum frequency and loss modulus was performed (Fig. 3). The observed scattering in data is well within the uncertainty in the loss modulus measurements giving the opportunity of the relaxation breadth comparison. As one can observe, the α -relaxation of the UPR is broader than HIPS. Nonetheless, the superposition of data points based on shift factor calculations by the WLF equation led to suitable results for the HIPS while failed for the UPR. The observed discrepancy in the UPR was attributed to its thermorheological complexity because of its dynamical heterogeneity at the studied temperatures. In other words, the glass transition of the matrix, polystyrene, and rigid gel particles, continuously crosslinked polyester by the polystyrene bridges, are quite similar. This complication has also been noted before for several polymers.^{21–23} Although, both studied systems were prepared via heterogeneous polymerization of styrene solution of either polybutadiene or polyester, morphologically, the final products are very different. In other words, HIPS is mainly composed of a polystyrene matrix filled with about 20% (v/v) stiff rubber particles. Although, the UPR is mainly formed by a thin polystyrene matrix, ligament, connecting micron-sized gels filled with continuously crosslinked polyester chains. Therefore, it could be said that in HIPS the dynamics of PS matrix is actually affected by the stiff rubber particles; however,

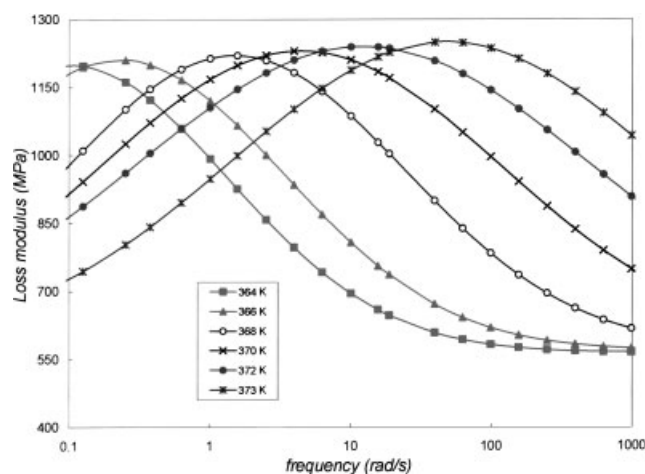


Figure 2 DMA isothermal curves for the UPR at different temperatures in the glass transition region.

in the UPR, the dynamics of glassy thin polystyrene ligament is superimposed on the microgels dynamics. It is due to the fact that two phases of HIPS differ in dynamics very much while the UPR shows very close T_g 's for both components.

The relaxation time can be defined as $\tau \equiv 1/\omega_{\max}$, where ω_{\max} is the frequency of the loss modulus maximum. This characteristic time corresponds to the most probable relaxation, and does not depend on any fitting function to the experimental data. The inset of Figure 4 shows the temperature-dependence of relaxation time for the HIPS and UPR, where curve fitted with the Vogel-Fulcher-Tammann (VFT) equation:^{24–26}

$$\tau = \tau_0 \exp\left(\frac{B}{T - T_\infty}\right) \quad (1)$$

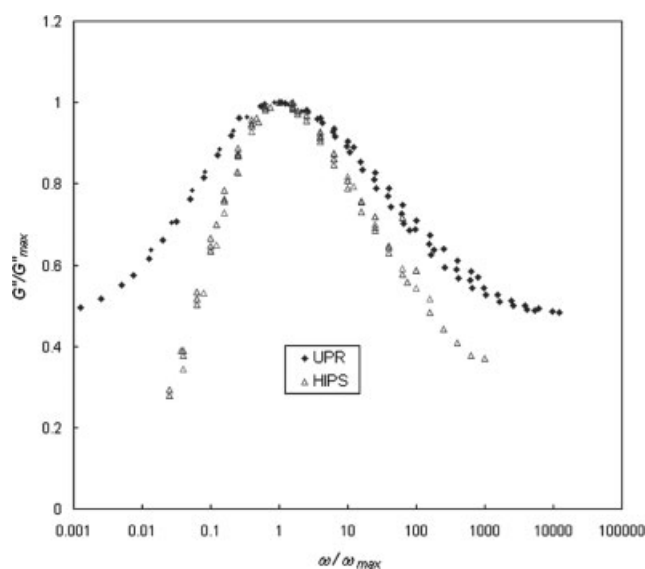


Figure 3 Normalized segmental loss dispersion peaks for the HIPS and UPR.

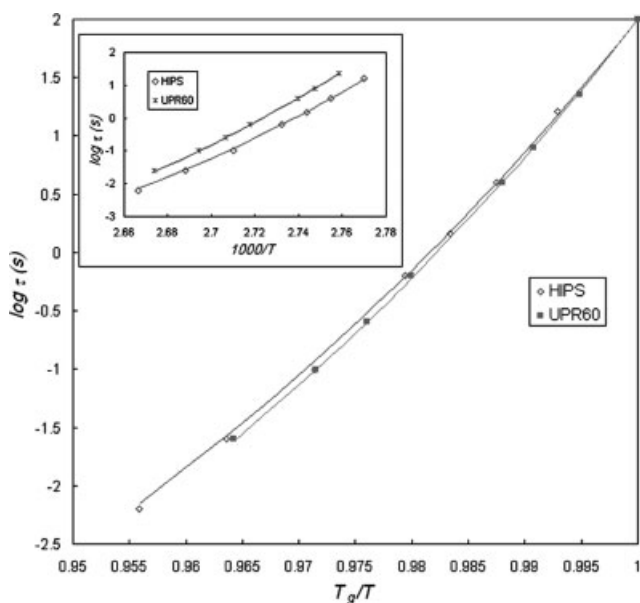


Figure 4 Fragility curves for the HIPS and UPR. The inset is temperature-dependence of segmental relaxation times for the HIPS and UPR. Solid lines are VFT fits to the data.

where B is a material parameter and T_∞ is Vogel temperature, which represents the point in which relaxation time diverges to infinity. According to Angell,²⁷ τ_0 is a characteristic time related to the frequency with which attempts for crossing some barrier opposing the particles rearrangement involved in relaxation occurs. In other words, τ_0 is the time a molecule needs to move into some free space expected to have phononlike scales, usually in the order of $\tau_0 = 10^{-14}$ s.²⁷ The VFT parameters of two samples were obtained using a nonlinear least squares fitting procedure (Table I).

The relaxation time data can be replotted based on a dimensionless temperature scale, T_g/T , fragility plot (Fig. 4). The T_g was defined as the temperature at which segmental relaxation time assumed a value of 100 s.^{7,9,12} It is clear that the variation of segmental relaxation time with respect to normalized temperature is steeper for the UPR in comparison with the HIPS. The evaluated slope of the plots at $T = T_g$ are called fragility, m , the quantity that could be calculated from VFT parameters too:²⁸

$$m = \left. \frac{d \log \tau}{d(T_g/T)} \right|_{T=T_g} = \frac{B/T_g}{\ln(10)} \left(1 - \frac{T_\infty}{T_g} \right)^{-2} \quad (2)$$

The value $m = 16$ corresponds to strong material limit (Arrhenius behavior) while for $m > 200$, the system reaches the fragility limit. The calculated m values were 122 and 128 for the HIPS and UPR, respectively, in agreement with the reported literature results for PS²⁹ and a UPR with slightly different structure.³⁰ Rather high fragility indices obtained for these materials categorize them as kinetically fragile systems.

It would be worth mentioning, however, that the direct comparison of two investigated systems does not represent the whole story. They were actually made through styrene polymerization in the presence of an unsaturated polymer namely polybutadiene or polyester. Even though, the aforementioned process led to the distribution of 1–5 μm secondary phase particles in polystyrene matrix, the overall and local compositions of the two systems were quite different. In other words, the HIPS composed of about 20% (v/v) of distributed stiff rubber particles while the UPR contained about 70% (v/v) of connected rigid particles. Therefore, the PS ligament in the UPR is much thinner than HIPS. Accordingly, the UPR is expected to be more fragile if its PS content enhances to a comparable composition with the HIPS. It is worth reminding that the main goal of this research has been to compare the role of stiff and rigid inclusions on the fragility of the same matrix, polystyrene, in two commercial products. In practice, however, large differences in PS ligament thickness and T_g overlap between the matrix and inclusions in the UPR led to the complexity of the comparison. Nonetheless, the thorough analysis of the extracted results showed still distinguishable differences between two investigated systems.

Breadth of relaxation function (Fig. 3) and temperature-dependency of relaxation times (Fig. 4) are generally correlated.³¹ Greater fragility is usually associated with a broader dispersion.³¹ On the basis of Ngai's coupling model,^{32,33} the broader α -dispersion of the UPR is a consequence of the intermolecular coupling enhancement among the relaxing moieties originated from the additional constraints imposed by crosslinking. The width of relaxation function is often quantified by fitting the modulus data using the Kohlrausch-Williams-Watts (KWW) equation:^{34,35}

$$G(t) = G_0 \exp \left[- \left(\frac{t}{\tau} \right)^{\beta_{\text{KWW}}} \right] \quad (3)$$

where $0 < \beta_{\text{KWW}} \leq 1$, τ is the KWW relaxation time, and G_0 is the glassy modulus. The β_{KWW} quantifies the relaxation time distribution and its width. In other words, β_{KWW} close to 0 implies a broad distribution while $\beta_{\text{KWW}} = 1$ represents narrow relaxation distribution.

To fit dynamic modulus data, they were converted from the frequency to the time scale using the follow-

TABLE I
The Best Fit Parameters of the VFT Equation on the HIPS and UPR Relaxation Data

System	τ_0 (K)	B (K)	T_∞ (K)	T_g (K)	$T_g - T_\infty$	m
HIPS	1×10^{-14}	1737	311	358	47	122
UPR	1×10^{-14}	1621	325	369	44	134

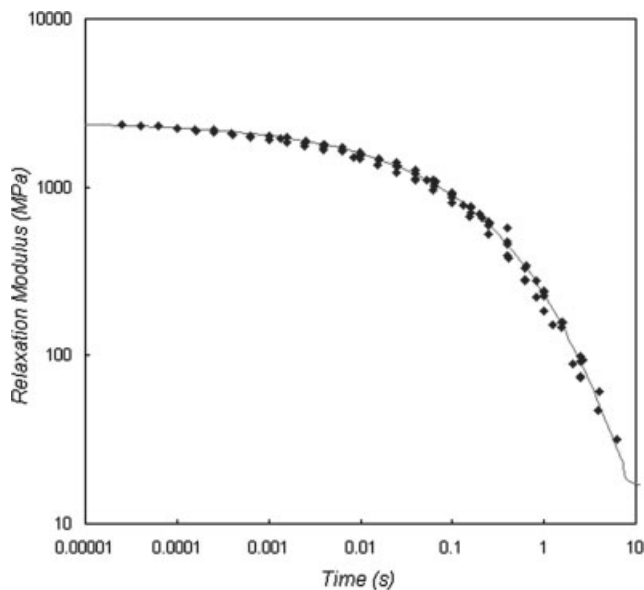


Figure 5 Time-temperature superposition for the HIPS. The solid line represents the KWW function fit to the data.

ing approximation:³⁶

$$G(t) = G'(\omega = 1/t) \quad (4)$$

Figure 5 shows the master curve for storage modulus of the HIPS as a function of $\log(t)$ and a reference temperature $T_{\text{ref}} = 369$ K. The master curve was constructed by applying time-temperature superposition principle. Finally, by fitting the KWW function to the obtained master curve, a value of $\beta_{\text{KWW}} = 0.37$ was determined. The relaxation width of the UPR, however, could not be quantified by the KWW equation; nonetheless, a lower value of β_{KWW} was expected. The thermorheologically complex state of the UPR dynamics at the investigated temperature window was proposed as the molecular mechanism of the observed heterogeneity.

Different segmental relaxation behavior of the HIPS and UPR can also be investigated based on the Angell's interpretation of fragility. As mentioned earlier, the glassy state of more fragile liquids corresponds to a wide variety of different structural arrangements, implying larger $\Delta C_p(T_g)$.^{10,11} Thus, many attempts have been done to find a correlation between the fragility and the cooperativity size at T_g . Both quantities, that is, $\Delta C_p(T_g)$ and the cooperativity length scale can be estimated from calorimetric experiments.

Here, we address this issue by determining and comparing the size of a cooperatively rearranging region (CRR), V_{CRR} , for both studied systems. Adam and Gibbs³⁷ defined CRR as a subensemble of particles, which can rearrange independently into a new configuration. The size of CRR is a measure of the length scale of cooperativity and closely related to its

corresponding glass transition temperature and relaxation time. Therefore, based on thermal fluctuation theory, Donth^{38,39} proposed an equation for calculating CRR at T_g , which its required data could be extracted from DSC experiments.

$$V_{\text{CRR}} = \xi_{\text{CRR}}^3 = k_B T_g^2 \Delta(1/C_v) / (\rho \delta T^2) \quad (5)$$

$$N_{\text{CRR}} = \frac{\rho N_A V_{\text{CRR}}}{M_m} \quad (6)$$

where V_{CRR} is the volume of a CRR, ξ_{CRR} is the characteristic length of cooperativity at T_g , k_B is the Boltzman constant, C_v is the specific heat capacity at constant volume, δT is the mean temperature fluctuation, N_{CRR} is the number of particles (monomer units) in a CRR, N_A is Avogadro number, ρ is the polymer density, and M_m is the molar mass of a particle. Glass transition was calculated by an equal-area construction about the heating curve using tangents from far below and far above T_g . In addition, Donth^{38,39} used the following approximation for calculating V_{CRR} from conventional DSC results. Donth^{38,39} approximated $\Delta(1/C_v)$ by $\Delta(1/C_p)$, which in turn is taken equivalent to $\Delta C_p/C_p^2$, where C_p is the specific heat capacity at con-

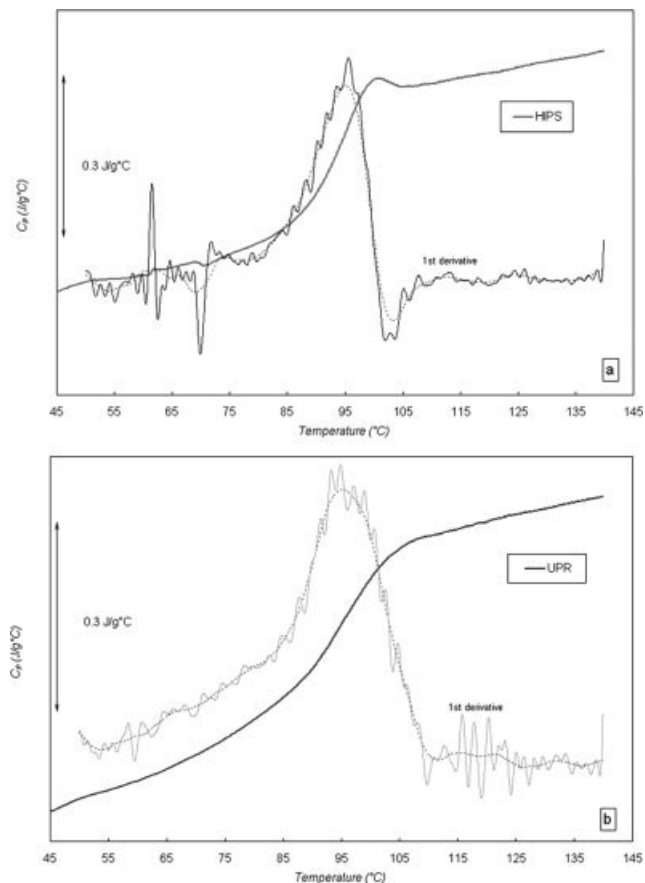


Figure 6 Specific heat capacities at constant pressure versus temperature for (a) the HIPS and (b) the UPR.

TABLE II
Sample Parameter Values Obtained From DSC for Calculation of V_{CRR}

System	ΔC_p (J/g K)	ΔC_p (J/mol K)	C_p (J/g K)	δT (K)	T_g (K)	V_{CRR} (nm ³)	N_{CRR}
HIPS	0.1936	20.1	1.4321	2.34	367	35.14	211
UPR	0.1935	177	1.3588	3.72	370	13.86	9.5

stant pressure, a quantity that is measured by DSC. The mean temperature fluctuation of one average CRR, δT , can be estimated by "a rule of thumb"⁴⁰: $\delta T = \Delta T/2.5$, where ΔT is the temperature interval where $C_p(T)$ varies between 16 and 84% of the total ΔC_p step at the glass transition. The DSC results for the investigated systems are provided in Figure 6 and Table II. The values of $\Delta C_p(T_g)$ for both studied samples are practically the same (0.2 J/g K). It was mentioned earlier that the main difference between the studied systems were the nature and the amount of their inclusions. Therefore, it was expected that the CRR size of polystyrene matrix in the HIPS sample increases in comparison with virgin PS because of the effect of stress field overlap of stiff rubber particles. On the other hand, the CRR size of polystyrene matrix in the UPR sample was anticipated much smaller. Therefore, normalizing $\Delta C_p(T_g)$ by the molecular weight of the structural units of the investigated systems proposed by Wunderlich⁴¹ leads to much higher values for the UPR, 170 in comparison with 20 J/mol K for the HIPS. This means that the UPR is both kinetically and thermodynamically more fragile than the HIPS. In other words, the mean volume of CRR is much larger for less fragile system (HIPS). Furthermore, a negative correlation between the fragility and the length scale of cooperativity was observed. This is in contrast to Kahle et al.⁴² and Solunov,⁴³ who reported a direct relation between fragility index and the volume of CRR and a linear correlation between fragility and the size of cooperative units for some polymers and inorganic super cooled liquids, respectively. Nonetheless, a direct correlation between two parameters has been doubted by Hempel et al.³⁹ The observed discrepancy could be attributed to the structural differences of two materials. The cured UPR with 60% (w/w) styrene is a highly crosslinked polymer. The average number of structural units between two consecutive junctions of this material was $v = 2.7$ from rubbery modulus measurements.⁴⁴ This is considerably smaller than the number of structural units of the UPR in its CRR at the glass transition. Consequently, the segmental motion in the UPR is affected with great restrictions imposed by network junctions. Nonetheless, the network heterogeneity with tight and loose regions led to broad relaxation times. On the other hand, the cooperative motions in the HIPS, although with a larger length scale, do not probably encounter considerable restrictions. Accordingly, the range of spatial restrictions or

confinements is of great importance when the correlation of fragility and CRR size are to be examined.

CONCLUSIONS

Segmental dynamics comparison of two reactively prepared polystyrene-based blends was performed by DMA and DSC analysis. Although, the HIPS sample was polystyrene consisted of dispersed 1–5 μm stiff rubbery particles, matrix of the UPR, polystyrene, contained the same size particles made of rigid highly crosslinked networks. The results were as follows. First, the dynamic fragility of the UPR was mildly higher than the HIPS system. However, the magnification in segmental dynamics differences would be expected if both systems with similar compositions, overall and locally, could be made. Second, the segmental dynamics data of the HIPS sample could be curve fitted to the KWW function with a $\beta_{\text{KWW}} = 0.37$. But, for the UPR, it could just be expected a lower value corresponding to experimentally observed broader dispersion. Finally, the fragility evaluation based on DSC thermograms showed comparable results. Nonetheless, normalization of the extracted data by molecular weight of the structural units of the two systems magnified their differences. The observed results could be interpreted based on the comparison of the cooperativity length scale and the scale of topological constraints.

The authors thank Dr. M. Karimi for his help on DMA and DSC experiments.

References

1. Eyring, H. *J Chem Phys* 1936, 4, 283.
2. Robertson, R. *J Chem Phys* 1966, 44, 3950.
3. Argon, A. *Philos Mag* 1973, 28, 839.
4. Malandro, D. L.; Lacks, D. J. *J Chem Phys* 1999, 110, 4593.
5. Nandagopal, M.; Utz, M. *J Chem Phys* 2003, 118, 8373.
6. Capaldi, F. M.; Boyce, M. C.; Rutledge, G. C. *Polymer* 2004, 45, 1391.
7. Ngai, K. L.; Plazek, D. *J Rubber Chem Technol* 1995, 68, 376.
8. Angell, C. A.; Ngai, K. L.; McKenna, G. B.; McMillan, P. F.; Martin, S. W. *Appl Phys Rev* 2000, 88, 3113.
9. Donth, E. *The Glass Transition: Relaxation Dynamics in Liquid and Disordered Materials*; Springer-Verlag: Berlin, 2001.
10. Angell, C. A. *Science* 1995, 267, 1924.
11. Angell, C. A. In *Structure and Properties of Glassy Polymers*; Tant, M. R., Hill, A. J., Eds.; American Chemical Society: Washington, DC, 1998, p 37.

12. Ngai, K. L.; Roland, C. M. *Macromolecules* 1993, 26, 6824.
13. Ngai, K. L.; Casalini, R.; Roland, C. M. *Macromolecules* 2005, 38, 4363.
14. Kumar, S. K.; Colby, R. H.; Anastasiadis, R. H. S. H.; Fytas, G. *J Chem Phys* 1996, 105, 3777.
15. Kamath, S.; Colby, R. H.; Kumar, S. K. *Macromolecules* 2003, 36, 8567.
16. Lodge, T. P.; McLeish, T. C. B. *Macromolecules* 2000, 33, 5278.
17. Leroy, E.; Alegria, A.; Colmenero, J. *Macromolecules* 2003, 36, 7280.
18. Lutz, T. R.; He, Y.; Ediger, M. D.; Pitsikalis, M.; Hadjichristidis, N. *Macromolecules* 2004, 37, 6440.
19. Delahaye, N.; Marais, S.; Saiter, J. M.; Metayer, M. J. *J Appl Polym Sci* 1998, 67, 695.
20. Hadi, Z. M. Sc. Thesis, Amirkabir University of Technology, 2002.
21. Plazek, D. J. *J Polym Sci Part A-2: Polym Phys* 1968, 6, 621.
22. Roland, C. M.; Ngai, K. L. *Macromolecules* 1992, 25, 363.
23. Ferri, D.; Castellani, L. *Macromolecules* 2001, 34, 3973.
24. Vogel, H. *Phys Z* 1921, 22, 645.
25. Fulcher, G. S. *J Am Ceram Soc* 1923, 8, 339.
26. Tammann, G.; Hesse, W. Z. *Anorg Allg Chem* 1926, 156, 245.
27. Angell, C. A. *Polymer* 1997, 38, 6261.
28. Hodge, I. M. *J Non-Cryst Solids* 1996, 202, 164.
29. Santangelo, P. G.; Roland, C. M. *Macromolecules* 1998, 31, 4581.
30. Saiter, A.; Bureau, E.; Zapolsky, H.; Marais, S.; Saiter, J. M. *J Non-Cryst Solids* 2002, 307-310, 738.
31. Bohmer, R.; Ngai, K. L.; Angell, C. A.; Plazek, D. J. *J Chem Phys* 1993, 99, 4201.
32. Ngai, K. L. *Comments Solid State Phys* 1979, 9, 127.
33. Ngai, K. L.; Plazek, D. J. *J Polym Sci Polym Phys Ed* 1986, 24, 619.
34. Kohlrausch, R. *Ann Phys* 1847, 12, 393.
35. Williams, G.; Watts, D. C. *Trans Faraday Soc* 1970, 66, 80.
36. Matsuoka, S. *Relaxation Phenomena in Polymers*; Hanser: New York, 1992.
37. Adam, G.; Gibbs, J. H. *J Chem Phys* 1965, 43, 139.
38. Donth, E. *J Polym Sci Polym Phys Ed* 1992, 34, 2881.
39. Hempel, E.; Hempel, G.; Hensel, A.; Schick, C.; Donth, E. *Phys Chem B* 2000, 104, 2460.
40. Donth, E.; Korus, J.; Hempel, E.; Beiner, E. *Thermochim Acta* 1997, 304/305, 239.
41. Wunderlich, B. *J Phys Chem* 1960, 64, 1052.
42. Kahle, S.; Korus, J.; Hempel, E.; Unger, R.; Horing, S.; Schröter, K.; Donth, E. *Macromolecules* 1997, 30, 7214.
43. Solunov, C. A. *Eur Polym J* 1999, 35, 1543.
44. Qazvini, N. T.; Mohammadi, N. *Polymer* 2005, 46, 9088.